

# UNC-80 and the NCA Ion Channels Contribute to Endocytosis Defects in Synaptojanin Mutants

Maelle Jospin,<sup>1</sup> Shigeki Watanabe,<sup>1,2</sup> Deepa Joshi,<sup>1</sup> Sean Young,<sup>1</sup> Kevin Hamming,<sup>3</sup> Colin Thacker,<sup>3</sup> Terrance P. Snutch,<sup>3</sup> Erik M. Jorgensen,<sup>1,2</sup> and Kim Schuske<sup>1,\*</sup>

<sup>1</sup>Department of Biology

<sup>2</sup>Howard Hughes Medical Institute  
University of Utah  
257 South 1400 East

Salt Lake City, UT 84112-0840

<sup>3</sup>Michael Smith Laboratories

University of British Columbia

Vancouver, British Columbia V6T 1Z3

Canada

## Summary

Synaptojanin is a lipid phosphatase required to degrade phosphatidylinositol 4,5 biphosphate (PIP<sub>2</sub>) at cell membranes during synaptic vesicle recycling [1, 2]. Synaptojanin mutants in *C. elegans* are severely uncoordinated and are depleted of synaptic vesicles, possibly because of accumulation of PIP<sub>2</sub> [2]. To identify proteins that act downstream of PIP<sub>2</sub> during endocytosis, we screened for suppressors of synaptojanin mutants in the nematode *C. elegans*. A class of uncoordinated mutants called “fainters” partially suppress the locomotory, vesicle depletion, and electrophysiological defects in synaptojanin mutants. These suppressor loci include the genes for the NCA ion channels [3], which are homologs of the vertebrate cation leak channel NALCN [4], and a novel gene called *unc-80*. We demonstrate that *unc-80* encodes a novel, but highly conserved, neuronal protein required for the proper localization of the NCA-1 and NCA-2 ion channel subunits. These data suggest that activation of the NCA ion channel in synaptojanin mutants leads to defects in recycling of synaptic vesicles.

## Results and Discussion

### *unc-80* Is a Suppressor of Synaptojanin Mutant Uncoordinated

Synaptojanin mutants accumulate PIP<sub>2</sub> [1] and have defects in synaptic vesicle endocytosis in mice, flies, and worms [1, 2, 5, 6]. To identify proteins that act downstream of PIP<sub>2</sub> during synaptic vesicle endocytosis, we screened for suppressors of synaptojanin mutants (*unc-26*) in *C. elegans*. In the screen, we identified *ox301*, an allele of the gene *uncoordinated-80* (*unc-80*). To quantify suppression, we performed race assays (Table 1; Figure S1 in the Supplemental Data available online). All three alleles of *unc-80* tested were able to suppress the locomotion defect of *unc-26* mutants (Table 1; Figure S1). In addition, mutations in *unc-80*

suppressed both a hypomorphic allele of *unc-26*(*e314*) and, to a lesser degree, a null allele of *unc-26*(*s1710*). Because *unc-80* mutations suppress both weak and null alleles of *unc-26*, it is likely that *unc-80* acts downstream, or in parallel to, synaptojanin.

One possible mechanism for suppression is that *unc-80* mutants could simply be hyperactive. However, *unc-80* mutants are not hyperactive; in fact, they are somewhat sluggish. *unc-80* mutants can move, but they generally spend their time lying still on the plate. If motivated by a sudden stimulus, animals move two body lengths and abruptly stop, in a phenotype called “fainting.” The fainting phenotype is still observed in *unc-26 unc-80* double mutants. Moreover, *unc-80* does not appear to nonspecifically increase neurotransmission, because it is not a general suppressor of synaptic transmission mutants (Table 1). In most cases, no strong genetic interactions were found between *unc-80* and other synaptic transmission mutants. The only consistent effect was that *unc-80* suppressed other mutations involved in PIP<sub>2</sub> metabolism. Endophilin (*unc-57*) binds synaptojanin and localizes it to membranes at synapses [5, 7–10]; perhaps not surprisingly, *unc-80* mutations also suppress the locomotory phenotype of *unc-57* mutants. PIP<sub>2</sub> is synthesized by the type 1 PIP kinase (*ppk-1* in *C. elegans*) [11, 12], and overexpression of PPK-1 causes an uncoordinated phenotype (D. Weinkove, M. Bastiani, and K.S., unpublished data). Again, mutations in *unc-80* suppress the locomotory phenotype of this strain. These data suggest that mutations in *unc-80* may be suppressing defects caused by the accumulation of PIP<sub>2</sub>.

### *unc-80* Encodes a Novel Conserved Protein

The uncoordinated phenotype of the *unc-80* mutation was mapped by single nucleotide polymorphisms to an interval on the right arm of chromosome V [13]. We used RNA interference in an RNAi-sensitized background (*eri-1 lin-15b*) [14] to screen candidate open reading frames for phenocopy of the *unc-80* behavioral defect [15]. We found that F25C8.3 gave a fainter phenotype similar to *unc-80* mutants. To show that F25C8.3 is indeed the *unc-80* locus, we rescued *unc-80* mutants with wild-type F25C8.3 DNA and identified the DNA lesion in six *unc-80* mutant alleles (Figure 1A; Figure S2, Table S1).

UNC-80 is a large protein with at least two isoforms (Figure S2; Wormbase). Domain and motif recognition programs failed to suggest a function for the predicted UNC-80 protein; however, it is highly conserved across its length to single proteins in other metazoans (Figure 1A). Thus, UNC-80 is the founding member of an evolutionarily conserved family of proteins.

### *unc-80* Is Expressed in Neurons

To determine in which cells *unc-80* is expressed, we placed GFP under the control of the *unc-80* promoter (*Punc-80:GFP*). The *unc-80* GFP reporter is broadly expressed in the nervous system (Figure 1B). The

\*Correspondence: schuske@biology.utah.edu

Table 1. Worm Race Locomotion Assay in Double Mutants

	Locus 1				
	Wild-Type	Synaptojanin Hypomorph <i>unc-26(e314)</i>	Synaptojanin Null <sup>a</sup> <i>unc-26(s1710)</i>	<i>unc-80 (ox301)</i>	<i>nca-2(gk5); nca-1(gk9)</i>
	99 ± 0.7, n = 3	16 ± 1.9, n = 15	1.2 ± 0.3, n = 13	90 ± 5.2, n = 3	98 ± 0.6, n = 3
Locus 2					
UNC-80: <i>unc-80(ox301)</i>	90 ± 5.2, n = 3	69 ± 6.2, n = 4; p < 0.0001	12.3 ± 3.3, n = 3; p < 0.0001		
UNC-79: <i>unc-79(e1068)</i>	83 ± 4.0, n = 3	53 ± 8.1, n = 3; p < 0.0001	6.9 ± 1.2, n = 7; p < 0.0001		
NCA channel: <i>nca-2(gk5); nca-1(gk9)</i>	98 ± 0.6, n = 3	80 ± 6.3, n = 5; p < 0.0001	12.7 ± 2.3, n = 8; p < 0.0001		
Ca <sub>v</sub> 2 Ca <sup>2+</sup> channel: <i>unc-2(lj1)</i>	56 ± 3.7, n = 8	0.0, n = 6 <sup>b</sup>		43 ± 5.4, n = 6; p = 0.6	
Ryanodine receptor: <i>unc-68(r1162)</i>	46 ± 11.2, n = 7	0.24 ± 0.24, n = 5; p = 0.0001		43 ± 12.4, n = 5; p = 0.8	
Ca <sub>v</sub> 1 Ca <sup>2+</sup> channel: <i>egl-19(n582)</i>	73 ± 4.1, n = 9	4.2 ± 0.96, n = 7; p = 0.0003		15 ± 2.5, n = 5; p < 0.0001	6.1 ± 3.5, n = 4; p < 0.0001
Syntaxin: <i>unc-64(e246)</i>	34 ± 4.6, n = 3	0.0, n = 3 <sup>b</sup>	0.0, n = 4 <sup>b</sup>	51 ± 1.7, n = 3; p = 0.02	
UNC-13: <i>unc-13(n2318)</i>	99 ± 0.0, n = 3	12 ± 3.7, n = 5; p = 0.32	0.2 ± 0.1, n = 3; p = 0.11		
Synaptotagmin: <i>snt-1(e2665)<sup>a</sup></i>	1.3 ± 0.9, n = 3			0.3 ± 0.3, n = 3; p = 0.35	
Phospholipase Cβ: <i>egl-8(sa47)</i>	69 ± 10.7, n = 3			52 ± 3.7, n = 3; p = 0.2	
AP180: <i>unc-11(e47)<sup>a</sup></i>	16 ± 2.5, n = 4			36 ± 6, n = 4; p = 0.02	
Endophilin: <i>unc-57(ok310)<sup>a</sup></i>	16 ± 3.1, n = 4			46 ± 5.6, n = 4; p = 0.0034	
Type 1 PIP kinase overexpression: <i>gqls25[Prab-3;PPK-1]</i>	17 ± 5.2, n = 5			75 ± 7.2, n = 5; p = 0.0002	

Double and triple mutants were constructed between the genotypes designated “locus 1” and “locus 2.” Percent of animals reaching the food ± SEM.

<sup>a</sup> 2 hr assays were used, all others are 1 hr.

<sup>b</sup> Unable to calculate p value because none of the double mutants arrived at the food.

reporter is expressed in both acetylcholine and GABA motor neurons as determined by double-labeling (Figure S3A). Although expression is observed in other tissues (Figure 1B), no expression was observed in the body muscle, suggesting that the uncoordinated phenotype is likely due to a loss of UNC-80 function in neurons.

#### UNC-80 Is Required for NCA-1 Localization or Stabilization in Axons

Only two other strains exhibit the fainter phenotype: animals lacking both subunits of a novel ion channel family encoded by the *nca-1* and *nca-2* genes [3], and animals lacking a large novel protein encoded by the *unc-79* gene [3, 16]. Fainter mutants have additional phenotypes in common. First, when placed in liquid, they are unable to swim, but instead become rigid and appear to have tremors (J. Pierce-Shimomura, personal communication; Table S1). Second, fainter mutants have altered sensitivity to volatile anesthetics such as halothane and enflurane [3, 16–18]. Third, *unc-79* mutants and *nca-1 nca-2* double mutants suppress the uncoordinated phenotype of animals lacking synaptojanin (Table 1; Figure S1). Together, these data suggest that UNC-80, UNC-79, and the NCA ion channels function in the same pathway.

Like *unc-80*, the *nca* genes are expressed in both excitatory and inhibitory motor neurons (Figures S3B and S3C). Interestingly, the mouse homologs of *unc-80*

(C030018G13) and of *nca* (A930012M17) also exhibit coincident expression patterns in the hippocampus, cerebellum, and piriform cortex (<http://www.brainatlas.org>) [19]. The coexpression and similar mutant phenotypes of the *unc-80* and *nca* genes suggest that these proteins may function together.

To determine whether *unc-80* is required for NCA localization, the distributions of the rescuing NCA-1::GFP and NCA-2::GFP fusion proteins (Table S1) were analyzed in *unc-80* mutants. In control animals, NCA-1::GFP and NCA-2::GFP are diffusely distributed along axons and do not appear to be enriched at synaptic sites (Figures 2A and 2B; Figures S3B, S3C, and S4A). In the absence of *unc-80*, axonal NCA-1::GFP and NCA-2::GFP expression is reduced in the axons of motor neurons (Figure S4A) and nerve ring (Figures 2A and 2B). Compared to wild-type levels, NCA-1::GFP and NCA-2::GFP levels in the nerve ring are reduced to 40% and 48%, respectively (Figure 2C). However, expression in cell bodies is not reduced, and may actually be increased, suggesting that NCA-1::GFP and NCA-2::GFP protein is still made in the absence of *unc-80*. By contrast, axonal fluorescence of the voltage-gated calcium channel (UNC-2::GFP), which is related to the vertebrate Ca<sub>v</sub>2 family of synaptic calcium channels, is not affected in *unc-80* mutants (Figure 2C; Figure S4B). Other synaptic components are also properly localized, including the synaptic vesicle proteins synaptobrevin

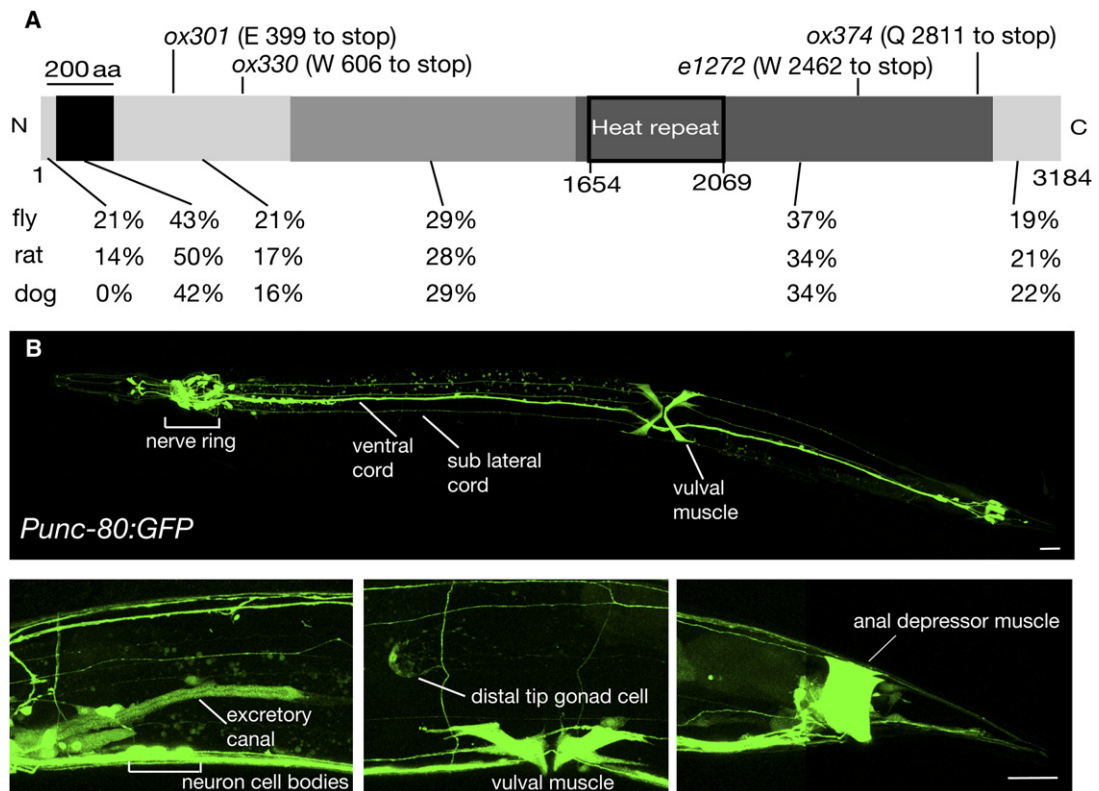


Figure 1. *unc-80* Encodes a Large, Conserved Neuronal Protein

(A) *unc-80* encodes a protein predicted to be 3184 amino acids in length (splice form F25C8.3a). Dark regions indicate strong conservation with homologs in other species. The percent identity between *C. elegans* and homologous proteins in *Drosophila* (CG18437-PA), rat (XP\_001053529), and canine (XP\_545626) for each of these regions is shown below. Partial sequences for mouse (XP\_898856) and human (C2orf21/EAW70465) also exist. A Heat domain was predicted by SMART, with a score of  $9 e^{-06}$ , but not by other domain search programs including Interpro and Motif scan.

(B) *unc-80* is strongly expressed in neurons. An adult hermaphrodite expressing *Punc-80::GFP* is shown, ventral side is up. Strong expression is observed in the nervous system and in the vulval muscle. Below are magnified images showing expression in the anterior excretory canal just posterior of the head, the vulval muscle, distal tip cell of the gonad, and the anal depressor muscle in the tail, lateral views. Scale bars represent 10  $\mu\text{m}$ .

and synaptotagmin and endocytic sites as marked by clathrin (Figures S4C and S4D). Thus, UNC-80 appears to be required for localization of NCA-1 and NCA-2 in the axon membrane, although we cannot rule out an additional role in channel function.

UNC-80 has a similar function as another protein UNC-79, which is required for maintaining NCA protein expression levels [3]. Therefore, in *C. elegans*, the normal function of the NCA ion channel requires two large proteins (UNC-79 and UNC-80) that contain no clear domains but are strongly conserved in all animals.

#### Restoration of Synaptic Vesicle Number in the Synaptojanin Mutants

Why does disruption of NCA channel function suppress synaptojanin mutant uncoordination? The most profound synaptic phenotype in *unc-26* mutants is that there are fewer synaptic vesicles [2]. To determine whether *unc-80* and *nca-1 nca-2* mutations suppress the synaptic vesicle depletion of *unc-26* mutants, we characterized the ultrastructure of synapses in these genotypes by a high-pressure freezing protocol. The number of synaptic vesicles in *unc-26(s1710)* mutants was reduced compared to the wild-type (Figure 3A; 42% in

acetylcholine neurons and 32% in GABA neurons). The remaining vesicles were often distributed at a distance from the presynaptic density arranged in a “string-of-pearls” (Figure 3B). The string-of-pearls phenotype of *unc-26* mutants was not suppressed by mutations in *unc-80* or *nca-1 nca-2* (Figure 3B). However, synaptic vesicle number in *unc-26 unc-80* double mutants, although still reduced compared to the wild-type (81% in acetylcholine and 60% in GABA neurons; Figure 3A), shows a significant improvement over *unc-26* mutants alone (1.9-fold and 1.8-fold more vesicles, respectively). Similar levels of suppression are observed in *nca-1 nca-2 unc-26* triple mutants (68% synaptic vesicles in acetylcholine neurons and 55% in GABA neurons compared to the wild-type; Figure 3A) but have 1.6-fold more synaptic vesicles in acetylcholine neurons and 1.7-fold more in GABA neurons than *unc-26(s1710)*. The increase in synaptic vesicle number suggests that the recycling defect in *unc-26* mutants is ameliorated by the loss of UNC-80 or NCA proteins.

Even in an otherwise wild-type background, *unc-80* and *nca-1 nca-2* mutants exhibit an increase in synaptic vesicle number at both acetylcholine (1.2-fold in *unc-80* and 1.2-fold in *nca-1; nca-2*) and GABA synapses

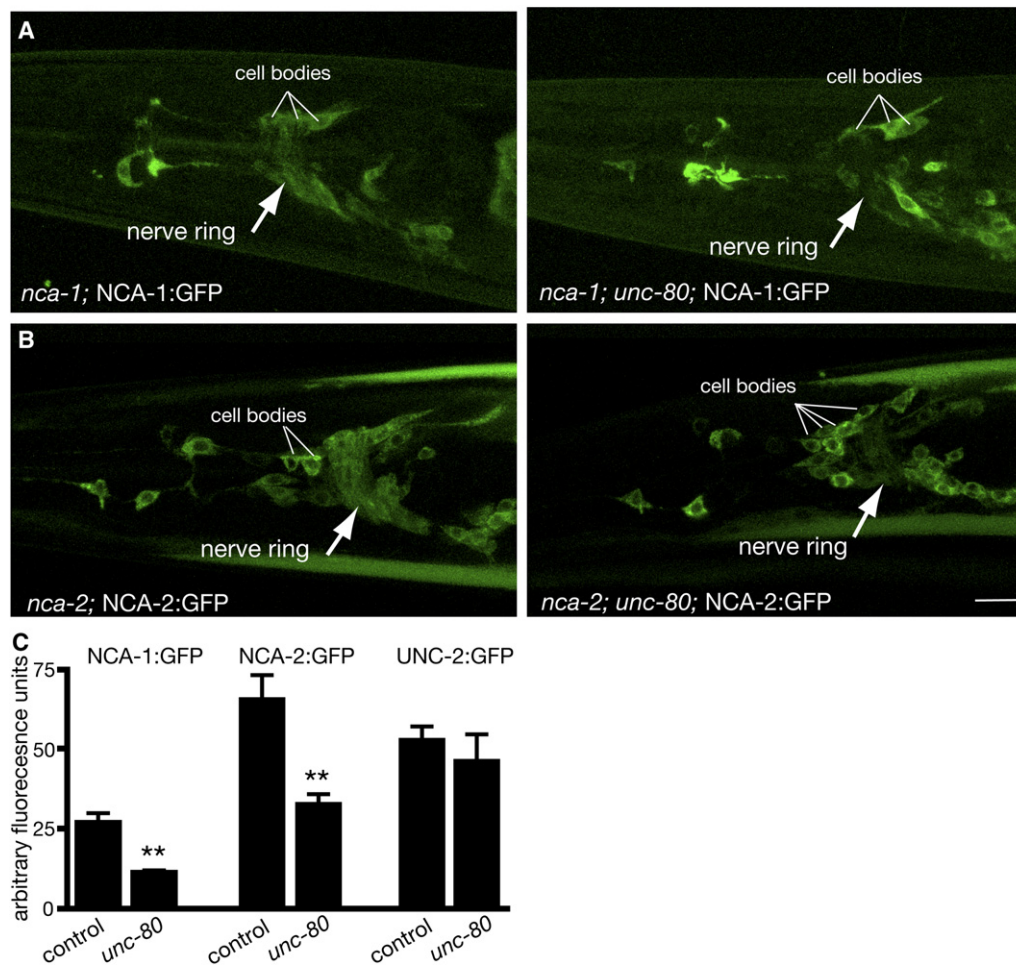


Figure 2. Localization of NCA-1 and NCA-2 Are Disrupted in *unc-80* Mutants

(A) NCA-1:GFP expression in the head of an *nca-1(gk9)* animal (left) and *nca-1(gk9); unc-80(ox301)* mutant (right).

(B) NCA-2:GFP expression in the head of an *nca-2(gk5)* animal (left) and *nca-2(gk5); unc-80(ox301)* mutant (right).

In (A) and (B), ventral is at the top, anterior to the left. Scale bar represents 10  $\mu$ m.

(C) Quantitative imaging of NCA-1:GFP, NCA-2:GFP, and UNC-2:GFP fluorescence in control and *unc-80(ox301)* animals. The right side of the nerve ring was imaged from the center of the pharynx to the hypodermis. Projected stacks, including the entire right side of the nerve ring, were used for quantification (average fluorescence intensity  $\pm$  SEM, n = animals): NCA-1:GFP (*vals46*): *nca-1(gk9)*,  $25.2 \pm 3.3$ , n = 5; *nca-1(gk9); unc-80(ox301)*,  $10.1 \pm 0.6$ , n = 4; p = 0.005, two-tailed, unpaired t test. A similar effect is seen for NCA-1:GFP (*vals46*) in a wild-type background, wild-type:  $28.4 \pm 3.2$ , n = 6; *unc-80(ox301)*:  $9.7 \pm 1.1$ , n = 6; p = 0.0003. NCA-2:GFP (*vals41*): *nca-2(gk5)*,  $64.7 \pm 8.0$ , n = 6; *nca-2(gk5); unc-80(ox301)*,  $31.4 \pm 3.2$ , n = 6; p = 0.003. UNC-2:GFP (*vals33*): *unc-2(e55)*,  $52.0 \pm 4.5$ , n = 5; *unc-2(e55); unc-80(ox301)*,  $44.7 \pm 8.7$ , n = 5; p = 0.48. \*\*p = 0.005–0.001.

(1.5-fold in *unc-80* and 1.2-fold in *nca-1; nca-2*) (Figure 3A). It is possible that *unc-80* and *nca-1 nca-2* suppress the synaptotagmin phenotype indirectly; that is, that mutating these genes leads to an increase in synaptic vesicle number in any genotype. However, the proportional change is much greater in the *unc-26* mutant background (Figure 3A), suggesting that the NCA channel function is reducing synaptic vesicle number because of the synaptotagmin mutant defect—perhaps because of inappropriate increases in PIP<sub>2</sub>.

#### Restoration of Synaptic Transmission in Synaptotagmin Mutants

Do mutations in *unc-80* and *nca-1 nca-2* alleviate the exocytosis defects observed in synaptotagmin mutants? We recorded miniature postsynaptic currents (“minis”) at neuromuscular junctions by using voltage-clamp

recordings from body muscle cells (Figures 3C and 3D). The frequency of minis in synaptotagmin null mutants is 17% compared to wild-type animals (0.5 mM calcium). The frequency of minis is increased by more than 2-fold in *unc-26(s1710) unc-80(ox301)* and *nca-1 nca-2 unc-26(s1710)* mutants, suggesting that loss of *unc-80* or *nca-1 nca-2* confers a significant improvement in synaptic transmission in the absence of synaptotagmin.

The fainter phenotype observed in *unc-80* and *nca-1 nca-2* mutants suggests that these mutants have a defect in synaptic transmission. In fact, these mutants exhibit a decrease in acetylcholine release as assayed by resistance to an inhibitor of acetylcholinesterase (Figure S5A). A defect in neurotransmission is not so apparent at an electrophysiological level. In low calcium (0.5 mM calcium), mini frequencies are normal in these strains (Figures 3C and 3D). By contrast, in high calcium

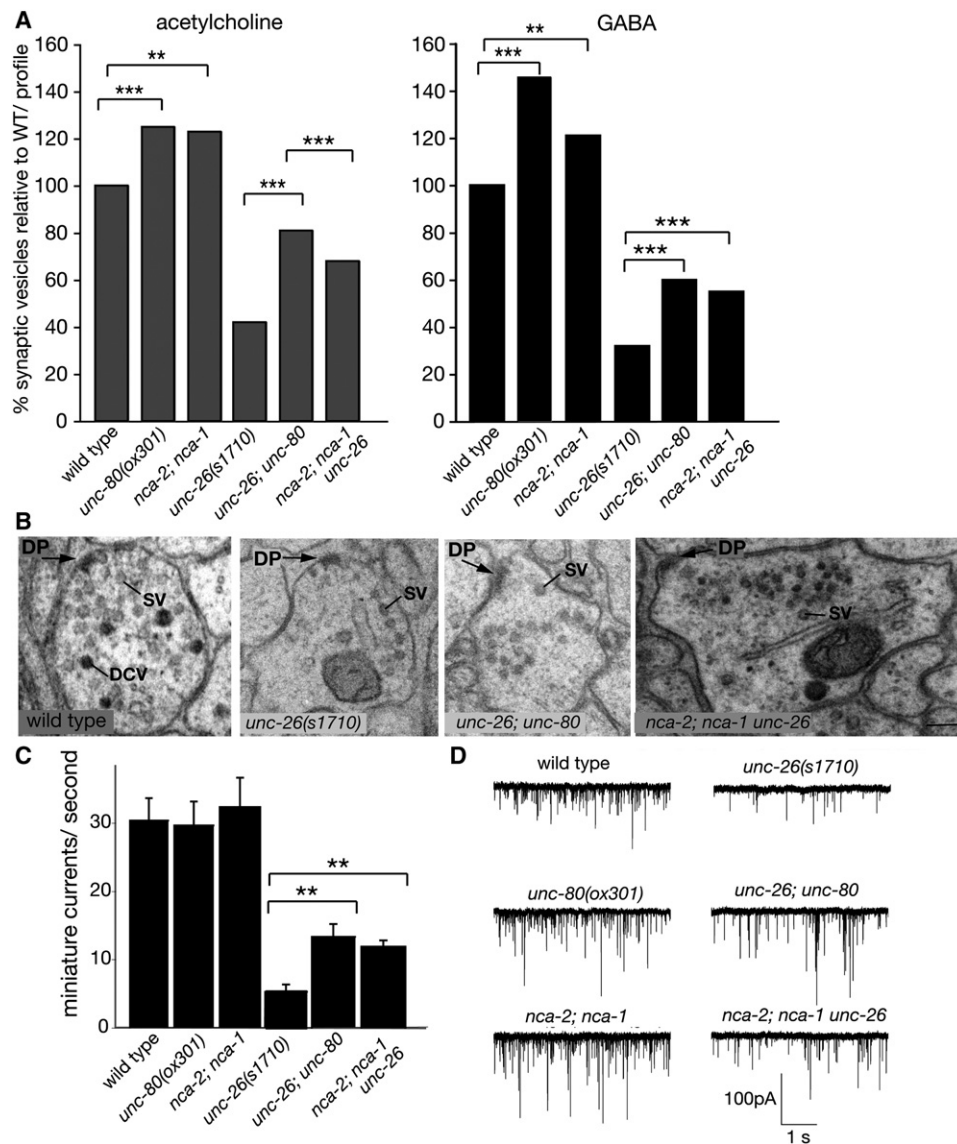


Figure 3. Suppression of Synaptojanin Mutant Phenotypes by *unc-80* and by *nca-1; nca-2*

(A) Vesicle number in mutants. The percent of synaptic vesicles per profile relative to the wild-type is shown. Average numbers of synaptic vesicles per profile were calculated for both acetylcholine and GABA neurons from two young adult hermaphrodites. Left, genotype acetylcholine synapses (number of synaptic vesicles per profile  $\pm$  SEM,  $n$  = synapses): wild-type ( $20.6 \pm 0.9$ ,  $n = 14$ ), *unc-80* ( $25.9 \pm 1.0$ ,  $n = 10$ ), *nca-2; nca-1* ( $25.4 \pm 1.4$ ,  $n = 8$ ), *unc-26(s1710)* ( $8.9 \pm 0.4$ ,  $n = 19$ ), *unc-26; unc-80* ( $16.7 \pm 1.1$ ,  $n = 10$ ), *nca-2; nca-1 unc-26* ( $14.1 \pm 1.0$ ,  $n = 10$ ). Right, genotype GABA synapses (number of synaptic vesicles per profile  $\pm$  SEM,  $n$  = synapses): wild-type ( $33.8 \pm 1.2$ ,  $n = 13$ ), *unc-80* ( $49.2 \pm 2.3$ ,  $n = 10$ ), *nca-2; nca-1* ( $40.8 \pm 2.6$ ,  $n = 10$ ), *unc-26* ( $10.9 \pm 0.6$ ,  $n = 17$ ), *unc-26; unc-80* ( $20.1 \pm 1.5$ ,  $n = 10$ ), *nca-2; nca-1 unc-26* ( $18.6 \pm 1.7$ ,  $n = 10$ ).  $p$  value calculated by two-tailed, unpaired  $t$  test. \*\* $p = 0.005$ – $0.001$ , \*\*\* $p < 0.001$ .

(B) Electron micrographs of profiles from acetylcholine neurons containing a dense projection (DP), arrows; lines indicate synaptic vesicles (SV) and dense core vesicles (DCV). Scale bar represents 100 nm.

(C) Frequency of miniature postsynaptic currents (minis) in the presence of 0.5 mM external calcium. Minis were recorded at a holding potential of  $-60$  mV on ventral medial body muscle cells. Minis per second  $\pm$  SEM,  $n$  = animals: wild-type ( $30.3 \pm 3.2$ ,  $n = 12$ ), *unc-80* ( $29.5 \pm 3.5$ ,  $n = 11$ ), *nca-2; nca-1* ( $32.2 \pm 4.3$ ,  $n = 8$ ), *unc-26(s1710)* ( $5.7 \pm 1.1$ ,  $n = 7$ ), *unc-26; unc-80* ( $13.3 \pm 1.9$ ,  $n = 7$ ), *nca-2; nca-1 unc-26* ( $11.8 \pm 1$ ,  $n = 7$ ).  $p$  value calculated by two-tailed, unpaired  $t$  test. \*\* $p = 0.005$ – $0.001$ .

(D) Representative traces recorded in 0.5 mM calcium.

(5.0 mM calcium), mini frequencies are more variable than in the wild-type (Figure S5B). Half of the cells exhibited very low mini frequencies (lower than 20 fusions per second) in *unc-80(ox301)*, in *unc-80(ox330)*, and in *nca-1 nca-2*, but not in wild-type animals (Figures S5C and S5D). These data suggest that increased extracellular calcium reduces the rate of synaptic vesicle release in *unc-80* and *nca-1 nca-2* mutants.

#### Models for *unc-80* and *nca-1 nca-2* Suppression of *unc-26*

How do mutations in *unc-80* and *nca-1 nca-2* suppress the depletion of synaptic vesicles in synaptojanin mutants? One possibility is that these mutations simply reduce exocytosis and thereby allow the crippled endocytic machinery time to catch up. As observed in ald-carb assays, *unc-80* and *nca-1 nca-2* mutants exhibit

a weak defect in exocytosis. If this model were true, then other mutants defective for exocytosis should also suppress *unc-26*. To test this hypothesis, we made double mutants between *unc-26* and mutations in genes that decrease but do not eliminate synaptic vesicle release. Such mutations did not suppress and in most cases exacerbated the synaptojanin mutant phenotype (Table 1), including mutations in the neural calcium channel  $Ca_v2$  (*unc-2*), the “long-lasting” calcium channel  $Ca_v1$  (*egl-19*), the ryanodine receptor (*unc-68*), and weak mutations in syntaxin (*unc-64*) and UNC-13 (*unc-13*). These data suggest that a general decrease in synaptic vesicle exocytosis is not sufficient to suppress *unc-26* uncoordination.

Another possibility is that the NCA channel function inhibits residual endocytosis of synaptic vesicles in *unc-26* mutants. In support of this model, absence of NCA channel function increases synaptic vesicle numbers in synaptojanin mutants. The increase in synaptic vesicles is mirrored by a proportional increase in synaptic vesicle exocytosis in the suppressed strain.

The original goal of this study was to identify proteins that act downstream of  $PIP_2$  accumulation at the synapse. Elimination of the synaptojanin  $PIP_2$  phosphatase or overexpression of the type 1  $PIP$  kinase would be expected to lead to an accumulation of  $PIP_2$ , and both strains generate uncoordinated animals. The uncoordinated phenotypes of both of these strains is suppressed by mutations in NCA channel function. Lipids, including  $PIP_2$ , regulate the activity of many ion channels [20]. Our data suggest that the NCA channel may be inappropriately activated by  $PIP_2$  and partially contributes to the synaptojanin mutant phenotype. Mislocalization of the NCA channels in *unc-80* mutants, or elimination of the channels themselves, partially alleviate this effect.

#### Supplemental Data

Five figures, one table, and Experimental Procedures are available at <http://www.current-biology.com/cgi/content/full/17/18/1595/DC1/>.

#### Acknowledgments

We would like to thank M. Zhen for the *nca-1 nca-2 unc-80* strain and for sharing unpublished data, P. Morgan for sharing unpublished data, J. Pierce-Shimomura for sharing *unc-80* mapping data, M. Alion for *unc-80(ox330)* and *unc-80(ox329)*, G. Holloper for the *Punc-17:mCherry* strain, M. Gu for the GFP-tagged synaptojanin strain, B. Grant, K. Sato, and M. Gu for the GFP-tagged clathrin strain, the *C. elegans* Genome Center for strains, and W. Davis for critical reading of the manuscript. Additionally, we would like to thank J. Weis, N. Jorgensen, and D. Lewis for technical assistance. The research was funded by grants from the National Institutes of Health (NS48391 to K.S., NS034307 to E.M.J.) and from the Lowe Syndrome Association and the Lowe Syndrome Trust to K.S. and E.M.J. E.M.J. is an Investigator of the Howard Hughes Medical Institute, T.P.S. is supported by an operating grant from the Canadian Institutes for Health Research and a Canada Research Chair, and M.J. is supported by a long-term fellowship from Human Frontier Science Program.

Received: May 11, 2007

Revised: August 2, 2007

Accepted: August 7, 2007

Published online: September 6, 2007

#### References

1. Cremona, O., Di Paolo, G., Wenk, M., Luthi, A., Kim, W.T., Takei, K., Daniell, L., Nemoto, Y., Shears, S.B., Flavell, R.A., et al. (1999). Essential role of phosphoinositide metabolism in synaptic vesicle recycling. *Cell* 99, 179–188.
2. Harris, T.W., Hartweg, E., Horvitz, H.R., and Jorgensen, E.M. (2000). Mutations in synaptojanin disrupt synaptic vesicle recycling. *J. Cell Biol.* 150, 589–600.
3. Humphrey, J.A., Hamming, K.S., Thacker, C.M., Scott, R.L., Sedensky, M.M., Snutch, T.P., Morgan, P.G., and Nash, H.A. (2007). A putative cation channel and its novel regulator: cross-species conservation of effects on general anesthesia. *Curr. Biol.* 17, 624–629.
4. Lu, B., Su, Y., Das, S., Liu, J., Xia, J., and Ren, D. (2007). The neuronal channel NALCN contributes resting sodium permeability and is required for normal respiratory rhythm. *Cell* 129, 371–383.
5. Verstreken, P., Koh, T.W., Schulze, K.L., Zhai, R.G., Hiesinger, P.R., Zhou, Y., Mehta, S.Q., Cao, Y., Roos, J., and Bellen, H.J. (2003). Synaptojanin is recruited by endophilin to promote synaptic vesicle uncoating. *Neuron* 40, 733–748.
6. Dickman, D.K., Home, J.A., Meinertzhagen, I.A., and Schwarz, T.L. (2005). A slowed classical pathway rather than kiss-and-run mediates endocytosis at synapses lacking synaptojanin and endophilin. *Cell* 123, 521–533.
7. Schuske, K.R., Richmond, J.E., Matthies, D.S., Davis, W.S., Runz, S., Rube, D.A., van der Bliek, A.M., and Jorgensen, E.M. (2003). Endophilin is required for synaptic vesicle endocytosis by localizing synaptojanin. *Neuron* 40, 749–762.
8. Micheva, K.D., Kay, B.K., and McPherson, P.S. (1997). Synaptojanin forms two separate complexes in the nerve terminal. Interactions with endophilin and amphiphysin. *J. Biol. Chem.* 272, 27239–27245.
9. Ringstad, N., Nemoto, Y., and De Camilli, P. (1997). The SH3p4/SH3p8/SH3p13 protein family: binding partners for synaptojanin and dynamin via a Grb2-like Src homology 3 domain. *Proc. Natl. Acad. Sci. USA* 94, 8569–8574.
10. de Heuvel, E., Bell, A.W., Ramjaun, A.R., Wong, K., Sossin, W.S., and McPherson, P.S. (1997). Identification of the major synaptojanin-binding proteins in the brain. *J. Biol. Chem.* 272, 8710–8716.
11. Ishihara, H., Shibasaki, Y., Kizuki, N., Katagiri, H., Yazaki, Y., Asano, T., and Oka, Y. (1996). Cloning of cDNAs encoding two isoforms of 68-kDa type I phosphatidylinositol-4-phosphate 5-kinase. *J. Biol. Chem.* 271, 23611–23614.
12. Loijens, J.C., and Anderson, R.A. (1996). Type I phosphatidylinositol-4-phosphate 5-kinases are distinct members of this novel lipid kinase family. *J. Biol. Chem.* 271, 32937–32943.
13. Davis, M.W., Hammarlund, M., Harrach, T., Hullett, P., Olsen, S., and Jorgensen, E.M. (2005). Rapid single nucleotide polymorphism mapping in *C. elegans*. *BMC Genomics* 6, 118.
14. Wang, D., Kennedy, S., Conte, D., Jr., Kim, J.K., Gabel, H.W., Kamath, R.S., Mello, C.C., and Ruvkun, G. (2005). Somatic misexpression of germline P granules and enhanced RNA interference in retinoblastoma pathway mutants. *Nature* 436, 593–597.
15. Kamath, R.S., Fraser, A.G., Dong, Y., Poulin, G., Durbin, R., Gotta, M., Kanapin, A., Le Bot, N., Moreno, S., Sohrmann, M., et al. (2003). Systematic functional analysis of the *Caenorhabditis elegans* genome using RNAi. *Nature* 421, 231–237.
16. Sedensky, M.M., and Meneely, P.M. (1987). Genetic analysis of halothane sensitivity in *Caenorhabditis elegans*. *Science* 236, 952–954.
17. Morgan, P.G., Sedensky, M.M., Meneely, P.M., and Cascorbi, H.F. (1988). The effect of two genes on anesthetic response in the nematode *Caenorhabditis elegans*. *Anesthesiology* 69, 246–251.
18. Morgan, P.G., Sedensky, M., and Meneely, P.M. (1990). Multiple sites of action of volatile anesthetics in *Caenorhabditis elegans*. *Proc. Natl. Acad. Sci. USA* 87, 2965–2969.
19. Lein, E.S., Hawrylycz, M.J., Ao, N., Ayres, M., Bensinger, A., Bernard, A., Boe, A.F., Boguski, M.S., Brockway, K.S., Byrnes, E.J., et al. (2007). Genome-wide atlas of gene expression in the adult mouse brain. *Nature* 445, 168–176.
20. Suh, B.C., and Hille, B. (2005). Regulation of ion channels by phosphatidylinositol 4,5-bisphosphate. *Curr. Opin. Neurobiol.* 15, 370–378.

# UNC-80 and the NCA Ion Channels Contribute to Endocytosis Defects in Synaptojanin Mutants

Maele Jospin, Shigeki Watanabe, Deepa Joshi, Sean Young, Kevin Hamming, Colin Thacker, Terrance P. Snutch, Erik M. Jorgensen, and Kim Schuske

## Supplemental Experimental Procedures

### *C. elegans* Strains

The wild strains used are Bristol N2 and Hawaiian CB4856. The strains used for phenotypic analysis are EG3039: *unc-26(e314)* IV, EG3027: *unc-26(s1710)* IV, EG4080: *unc-80(ox301)* V, EG4071: *unc-80(ox330)* V, CB1272: *unc-80(e1272)* V, EG2710: *unc-57(ok310)* I, UF62: *gqls25[Prab-3:PPK-1; lin-15+] I; oxls12[Punc-47:GFP] lin-15(n765ts)* X, CB47: *unc-11(e47)* I, EG1055: *unc-64(e246)* III, MT6977: *snt-1(n2665)* II, JT47: *egl-8(sa47)* V, AQ130: *unc-2(lj1)* X, MT1212: *egl-19(n582)* IV, TR2171: *unc-68(r1162)* V, EG3804: *nca-2(gk5)* III; *nca-1(gk9)* IV, EG3524: *unc-26(e314)* IV; *unc-80(ox301)* V, EG3492: *unc-26(s1710)* IV; *unc-80(ox301)* V, EG4151: *unc-26(e314)* IV; *unc-80(ox330)* V, EG3511: *unc-26(e314)* IV; *unc-80(e1272)* V, EG3504: *unc-57(ok310)* I; *unc-80(ox301)* V, EG3934: *gqls25[Prab-3:PPK-1; lin-15+] I; unc-80(ox301)* V; *lin-15(n765ts)* X; *oxls12[Punc-47:GFP; lin-15+] X*, EG3881: *unc-11(e47)* I; *unc-80(ox301)* V, EG3533: *unc-64(e264)* III; *unc-80(ox301)* V, EG3626: *snt-1(n2665)* II; *unc-80(ox301)* V, EG3753: *egl-8(sa47)* *unc-80(e1272)* V, EG3975: *unc-80(ox301)* V; *unc-2(lj1)* X, EG4078: *egl-19(n582)* IV; *unc-80(ox301)* V, EG4069: *unc-68(r1162)* *unc-80(ox301)* V, EG4070: *nca-2(gk5)* III; *nca-1(gk9)* *unc-26(s1710)* IV, EG4153: *unc-26(e314)* IV; *unc-2(lj1)* X, EG4157: *unc-26(e314)* IV; *unc-68(r1162)* V, EG3972: *egl-19(n582)* *unc-26(e314)* IV, EG4155: *egl-19(n582)* IV; *unc-2(lj1)* X, EG4156: *egl-19(n582)* IV; *unc-68(r1162)* V. The *unc-80* rescued strains are EG4667: *unc-80(ox301)* V; *oxEx1020[unc-80 rescue, myo-2:GFP]*, and EG4668: *unc-80(ox301)* V; *oxEx1021[unc-80 rescue, myo-2:GFP]*. GFP-expressing strains are as follows: TS469: *nca-2(gk5)* III; *nca-1(gk9)* IV; *vals46[Pnca-1:NCA-1:GFP, lin-15+]*; *lin-15(n765ts)* X, TS465: *nca-2(gk5)* III; *nca-1(gk9)* IV; *vals41-[Pnca-2:NCA-2:GFP, lin-15+]*; *lin-15(n765ts)* X, EG4669: *vals46-[Pnca-1:NCA-1:GFP, lin-15+]*, EG4670: *unc-80(ox301)* V; *vals46-[Pnca-1:NCA-1:GFP, lin-15+]*. TS337: *vals33[UNC-2:GFP; lin-15+]*; *unc-2(e55)* X and EG4666: *vals33[UNC-2:GFP; lin-15+]*; *unc-80(ox301)* V; *unc-2(e55)* X. The *unc-80* GFP reporter strain is EG4561: *oxEx839[Punc-80:GFP, lin-15+]*; *lin-15(n765ts)* X. The mRFP-marked GABA neuron strains are EG3832: *oxls215[Punc-47:mRFP, lin-15+]*; *lin-15(n765ts)* X and EG4338: *oxls215[Punc-47:mRFP, lin-15+] V; lin-15(n765ts)* X; *oxEx839[Punc-80:GFP, lin-15+]*. The mCherry-marked acetylcholine neuron strains are EG4558: *lin-15(n765ts)* X; *oxEx838[Punc-17:mCherry, lin-15+]*. EG4337: *lin-15(n765ts)* X; *oxEx838[Punc-17:mCherry, lin-15+]*; *oxEx839[Punc-80:GFP, lin-15+]*. The synaptojanin (VAMP):GFP strains are EG3540: *unc-80(ox301)* V; *lin-15(n765ts)* *nls52[VAMP:GFP, lin-15+] X*, MT8247: *nls52[VAMP:GFP, lin-15+]* *lin-15(n765ts)* X. The synaptojanin:GFP strains are EG3855: *lin-15(n765ts)* *oxls224[Punc-47:GFP::SNT-1, lin-15+] X* and EG4002: *unc-80(ox301)* V; *oxls224* X. The clathrin heavy chain:GFP strains are EG3438: *oxls174[clathrin:GFP, lin-15+] lin-15(n765ts)* X and EG3539: *unc-80(ox301)* V; *oxls174 lin-15(n765ts)* X. The *Punc-47:GFP* strains are EG3760: *unc-80(ox301)* V; *oxls12 lin-15(n765ts)* X and EG1306: *oxls12 lin-15(n765ts)* X.

### Behavioral Assays

#### Worm Race

Worms were fed OP50 bacteria and grown until most of the worms on a plate were adults. Strains were blinded and worms were washed off the plate with M9 media into 1.5 ml eppendorf tube and allowed to settle to bottom. Worms were washed two more times, and then 10  $\mu$ l (approximately 100–200 animals) of worms were placed in the center of a 10 cm plate containing normal worm media (NGM) and a 3.7 cm ring of HB101 bacteria that had grown overnight at 37°C. Animals were allowed to migrate 1–2 hr to the bacteria depending on the severity of the strain. Time started as soon as the M9 media had

evaporated. 1 hr: *unc-26(e314)*, *gqls25(Prab-3:PPK-1OE)*, *unc-64(e264)*, *egl-8(sa47)*, *unc-2(lj1)*, *egl-19(n582)*, *unc-68(r1162)*. 2 hr: *unc-26(s1710)*, *unc-57(ok310)*, *unc-11(e47)*, *snt-1(n2665)*. The number of adult animals reaching the bacteria was scored every 15 min and a final percent was calculated at the end of the assay. p values were calculated with two-tailed, unpaired t test.

#### Swimming Assay

A single worm was placed in a drop of M9 media on a plate containing NGM. The worm was allowed to recover from the transfer for 30 s, and then the number of times the worm bent its body to one side were counted for 2 min.

### *unc-80* Cloning

#### Mapping

*unc-80* had been previously mapped to the right side of chromosome V (M. Sedensky and P. Morgan, personal communication). To map the *unc-80(ox301)* locus, we used single-nucleotide polymorphisms between the wild-type Bristol strain and the wild-type Hawaiian CB4856 strain. Mapping was performed as previously described [S1]. In brief, Hawaiian CB4856 males were crossed to *unc-80(ox301)* hermaphrodites. From the F2 generation, 400 fainter animals were picked to individual plates. After 5 days, self progeny were washed from each plate with 200  $\mu$ l of water and placed in a single well of a 96-well plate. After worms settled to the bottom of the wells, 170  $\mu$ l of excess water was removed to leave 30  $\mu$ l in each well. The plates were frozen at  $-80^{\circ}\text{C}$ , and then 10  $\mu$ l of 4 $\times$  lysis buffer (200 mM KCl, 40 mM Tris [pH 8.3], 10 mM MgCl<sub>2</sub>, 1.8% NP40, 1.8% Tween 20, 0.04% (w/v) gelatin, 240  $\mu$ g/ml proteinase K) was added to each well to give 1 $\times$  lysis buffer. The worms were lysed by incubation at 65°C, 1 hr and 95°C, 15 min. Four single-nucleotide polymorphisms were used to fine-map the location of *unc-80*. From left to right: Y17D7B (flanking primers, 5'-GAAATTC AAATTTTGGAGAAACC-3' and 5'-TTCAGACCAATTTTGAATATTTA GG-3'), ZC15 (flanking primers, 5'-ACAGTCACCAAGAGTTTTTGC-3' and 5'-TCTTAAAAACGGGCGAGAATTAC-3'), F46B3 (flanking primers, 5'-GAACGCAGTGAGATCCGTTA-3' and 5'-TGTCGCTCCGATTGAA TGTA-3'), and T03D8 (flanking primers, 5'-TTCACCCATGTTGGTT ACGC-3' and 5'-ACTCTATTGGCGGACGACAC-3'). PCR was performed as previously described [S1], each well of the 96-well plate received 9.8  $\mu$ l of a PCR mix containing 8.5  $\mu$ l water, 1  $\mu$ l 10 $\times$  buffer, 0.2  $\mu$ l of 10 mM dNTP, 0.02  $\mu$ l of each primer (100  $\mu$ M), and 0.06  $\mu$ l Taq (5 units/ $\mu$ l). Templates were then pin-replicated from the lysis plate. PCR reactions were done with the cycling conditions: 2 min 94°C, 35 cycles of (15 s 94°C, 45 s primer-specific temperature, 1 min 72°C), 5 min 72°C. Annealing step was done at different temperatures depending on primer set: Y17D7B at 58°C, ZC15 at 52°C, F46B3 at 58°C, and T03D8 at 50°C. After amplification, PCR products were digested in the plate with restriction enzymes and fragments were run on a 2% agarose gel to assay for Hawaiian DNA banding pattern, suggestive of a recombinant. Y17D7B *Dral*: Bristol 324 bp and 164 bp, Hawaiian 488 bp. ZC15 *BstBI*: Bristol 299 bp and 144 bp, Hawaiian 443 bp. F46B3 *AluI*: Bristol 185 bp and 147 bp, Hawaiian 332 bp. T03D8 *Dral*: Bristol 474 bp and Hawaiian 290 bp and 184 bp. Of the 400 fainter animals cloned, 35 were recombinant for Y17D7B, 0 for F46B3, and 0 for T03D8. Only 1 of 26 Y17D7B recombinants was also recombinant for ZC15, suggesting that ZC15 marks the left breakpoint of the genetic region. The data suggested that *unc-80* mapped between ZC15 and the end of the chromosome because a right breakpoint could not be identified.

#### RNA Interference

There were 123 predicted open reading frames identified by Wormbase between ZC15 and the end of the chromosome. Sixty of these open reading frames were represented by RNAi clones [S2]. RNA

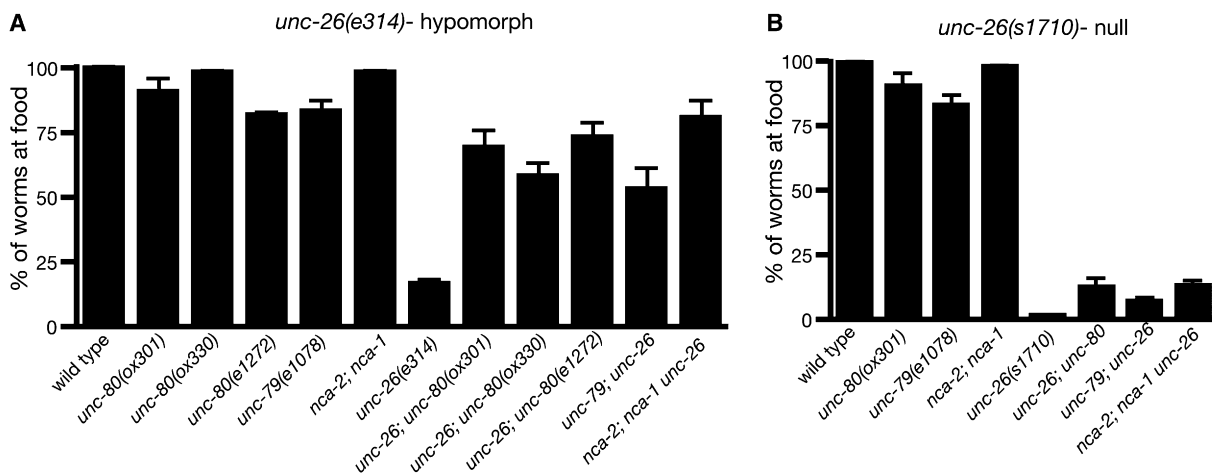


Figure S1. Genetic Interactions between Fainter Mutants and Synaptojanin Mutants

(A) Multiple alleles of *unc-80* as well as *unc-79* and *nca-2; nca-1* strongly suppress the uncoordinated phenotype of animals with a hypomorphic allele of *unc-26(e314)*. Percent of worms reaching the food after 1 hr ± SEM: wild-type 99 ± 0.7, *unc-80(ox301)* 90.3 ± 5.2, *unc-80(ox330)* 98.0 ± 1.0, *unc-80(e1272)* 81.3 ± 0.9, *unc-79(e1068)* 83.0 ± 4.0, *nca-2(gk5); nca-1(gk9)* 98.0 ± 0.6. For *unc-26(e314)* 16.1 ± 1.9, *unc-26(e314); unc-80(ox301)* 69 ± 6.2, *unc-26(e314); unc-80(ox330)* 57.6 ± 5.3, *unc-26(e314); unc-80(e1272)* 73.0 ± 5.1, *unc-79(e1068); unc-26(e314)* 52.7 ± 8.1, *nca-2(gk5); nca-1(gk9) unc-26(e314)* 80.8 ± 6.3. For all comparisons between *unc-26(e314)* and *unc-26(e314)* fainter double mutant combinations,  $p < 0.0001$ .  $p$  values were calculated by a two-tailed unpaired  $t$  test.

(B) Mutations in *unc-80*, *unc-79*, and the *nca* ion channel subunits suppress the strong allele of *unc-26(s1710)*. Percent of worms reaching the food after 1 hr ± SEM: *unc-26(s1710)* 1.2 ± 0.3, *unc-26(s1710); unc-80(ox301)* 12.3 ± 3.3, *unc-79(e1068); unc-26(s1710)* 6.9 ± 1.2, *nca-2(gk5); nca-1(gk9) unc-26(s1710)* 12.7 ± 2.3. For all comparisons between *unc-26(s1710)* and *unc-26(s1710)* fainter double mutant combinations,  $p < 0.0001$ .  $p$  values were calculated with a two-tailed unpaired  $t$  test.

interference feeding assays were performed as previously described [S2]. In brief, 2 ml cultures of RNAi bacteria in LB with 50 mg/ml ampicillin were grown overnight at 37°C. A drop of cultured bacteria was plated on standard NGM worm plates supplemented with a final concentration of 25 µg/ml carbenicillin and 1 mM IPTG. Two plates were made for each set of bacteria. The bacteria was allowed to grow overnight at room temperature, and five *eri-1 lin-15b* worms were plated on each of the duplicate plates. Plates were kept at room temperature for 3–4 days and the next generation was assayed for both the fainter and swimming phenotypes. Twenty-five of the sixty RNAi clones were tested and F25C8.3 was the only one to have a phenotype similar to *unc-80*.

#### Rescue

For injection rescue of *unc-80* mutants, three overlapping PCR fragments were amplified from genomic DNA and co-injected into *unc-80(ox301)*: fragment 1 (primers: 5'-GATATCCGCATATTGAGAGCTTAG-3' and 5'-GCAGTGTTTTATCTCTGAGGCTC-3') at 5 ng/µl, fragment 2 (primers: 5'-AGCATGTGAAGTGGTCTGTTG-3' and 5'-CGTGGTTCAAAGATGCAATCG-3') at 2.9 ng/µl, fragment 3 (primers: 5'-CCGGGTGCTCAATCCAAAAG-3' and 5'-CAGAATGCAGTCC TAATATGCCGA-3') at 5 ng/µl, and marker DNA *Pmyo-2:GFP* at 1.5 ng/µl. Fragments 1 and 2 overlap by 0.9 kb and fragments 2 and 3 overlap by 1.9 kb. Two independent lines were obtained in which animals were rescued for the fainter and swimming defects (extrachromosomal array alleles: *oxEx1020* and *oxEx1021*).

Domain search programs used: PsortII (<http://psort.ims.u-tokyo.ac.jp/>) [S3], Tmpred ([http://www.ch.embnet.org/software/TMPRED\\_form.html](http://www.ch.embnet.org/software/TMPRED_form.html)), TMHMM (<http://www.cbs.dtu.dk/services/TMHMM-2.0/>), SMART (Simple Modular Architectural Research Tools: <http://smart.embl-heidelberg.de>) [S4, S5], InterPro (<http://www.ebi.ac.uk/InterProScan>), and motif scan ([http://myhits.isb-sib.ch/cgi-bin/motif\\_scan](http://myhits.isb-sib.ch/cgi-bin/motif_scan)).

InterPro (<http://www.ebi.ac.uk/InterProScan>), and motif scan ([http://myhits.isb-sib.ch/cgi-bin/motif\\_scan](http://myhits.isb-sib.ch/cgi-bin/motif_scan)).

#### DNA Constructions

##### *unc-80 Promoter Fusion*

The *unc-80* promoter GFP expression construct was made by a PCR fusion-based approach [S6]. Specifically, the *unc-80* promoter was amplified from genomic DNA with the following primers: "U80A2" 5'-GATATCCGCATATTGAGAGCTTTAG-3' and "U80B" 5'-CCCTTACTCATTTTTTCTACCGGTACcaatggcactgaatcattctc-3'. GFP sequence was amplified with primers "U80C" 5'-GTACCGGTAGAAAATGAGTAAAGG-3' and "U80D" 5'-AAGGGCCCGTACGGCCGACTAGTAGG-3'. The two fragments were mixed together and then PCR was performed with the outside primers, "U80A" and "U80D." The PCR fragment was injected into *lin-15(n765ts)* mutants at 5 ng/µl with EK L15 [S7] (60 ng/ul). Three lines were obtained that had similar expression, and the analyzed array is *oxEx839*.

##### *Pnca-1:NCA-1:GFP Fusion*

This fusion construct was generated from three overlapping long-range PCR fragments. The first two products (overlapping fragments encompassing the entire *nca-1* locus) were amplified with wild-type genomic DNA as template. The first product contained the promoter and the 5' half of the gene. The first product (11907 bp) was generated with the sense primer N1GR1 (5'-GATATTGCTCCGTAGAGT

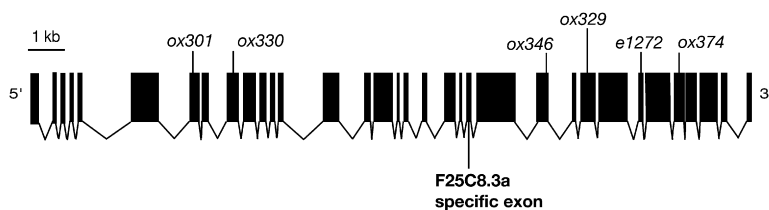


Figure S2. Predicted Gene Structure of *unc-80*

Wormbase: <http://www.wormbase.org>. F25C8.3a and F25C8.3b differ by the 9 amino acid exon 22, as shown. Amino acids are numbered with F25C8.3a. *ox301* (C to T, E399stop) induced by ENU (ethyl nitrosourea, Sigma), *ox330* (G to A, W606stop) induced by ENU (M. Alion), *e1272* (G to A, W2462stop) induced by EMS (J. Lewis), *ox374* (C to T, Q2811stop) induced by EMS (J. Park, background mutation in MT2612 *unc-8(n491n1193)*) led to early stop codons. *ox346* (G to A) disrupts the conserved G in the splice donor site of exon 24 induced by ENU (K. Schuske). *ox329* is a 22 bp deletion leading to a frame shift after amino acid A2116 and then a stop codon (ACCTGC [del GCCTATGTGAGAGACTATTACT] TCTTTCAT, 9 aa then stop) induced by ENU (M. Alion).

induced by EMS (J. Lewis), *ox374* (C to T, Q2811stop) induced by EMS (J. Park, background mutation in MT2612 *unc-8(n491n1193)*) led to early stop codons. *ox346* (G to A) disrupts the conserved G in the splice donor site of exon 24 induced by ENU (K. Schuske). *ox329* is a 22 bp deletion leading to a frame shift after amino acid A2116 and then a stop codon (ACCTGC [del GCCTATGTGAGAGACTATTACT] TCTTTCAT, 9 aa then stop) induced by ENU (M. Alion).

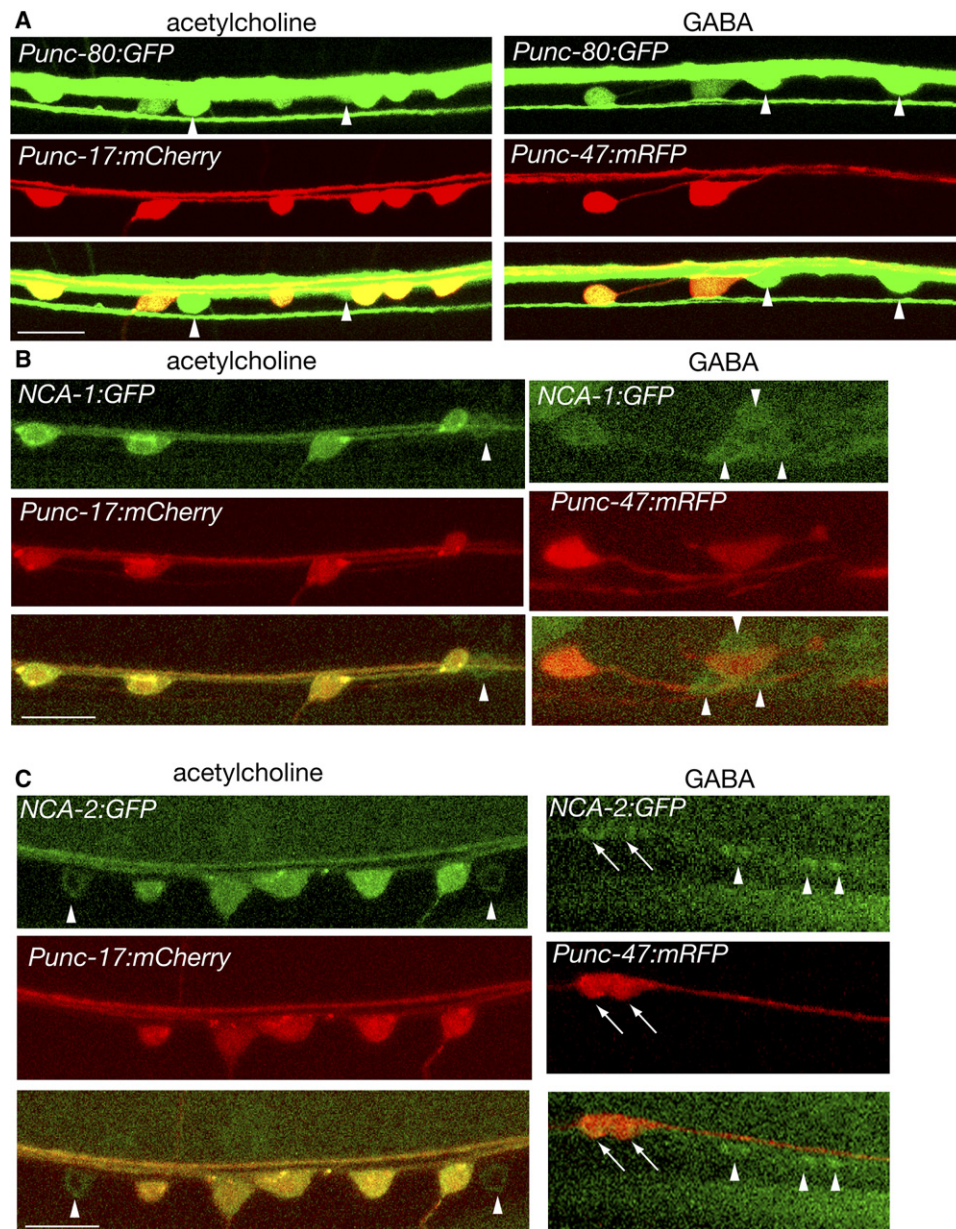


Figure S3. *nca-1* and *nca-2* Are Expressed in Acetylcholine and GABA Motor Neurons

(A) *Punc-80::GFP* in the ventral nerve cord has overlapping expression with acetylcholine neurons (*Punc-17::mCherry*) and GABA neurons (*Punc-47::mRFP*).

(B) *NCA-1::GFP* in the ventral nerve cord has overlapping expression with *Punc-17::mCherry* acetylcholine neurons and in the head *Punc-47::mRFP* GABA neurons.

(C) *NCA-2::GFP* in the ventral nerve cord has overlapping expression with *Punc-17::mCherry* acetylcholine neurons and *Punc-47::mRFP* GABA neurons. Arrows mark *NCA-2::GFP*- and *Punc-47::mRFP*-positive cells. The high background in images is due to the high laser intensity required to visualize the weak GFP expression. GFP-only neurons are GABA (left) and acetylcholine (right) neurons (arrowheads). Scale bars represent 10  $\mu$ m.

AG-3'), approximately 5.8 kb upstream of the first exon and the anti-sense primer N1GR2 (5'-TCAGATGGTCTTGAGAGTC-3'), located in exon 14. The second product extended from the end of exon 11 to the predicted stop codon. The second product (9164 bp) was amplified with the sense primer N1GR3 (5'-GATGTCATTGAATCCGGTTG-3') and the antisense primer N1GR5 (5'-CTTTGGCCAA TCCCGGGATCATCAACAAGGGAATCCACC-3') that contained GFP sequence at its 5' end (at the carboxy terminus of the NCA-1 protein). The third PCR product (1974 bp) amplified the GFP sequence from the plamid pPD95.75 (provided by A. Fire) with the sense primer N1GR6 (5'-GGTGGAAATCCCTTGTTGATGATCCCCGGGATTGGCCAAAG-3') that contained *nca-1* sequence at its 5'

end and the primer GFP3' (5'-ATCCGCTTACAGACAAGCTG-3'). Equimolar amounts of the 3' *nca-1* (second) and GFP (third) PCR products were then fused by PCR stitching resulting in an in-frame carboxy-terminal translational fusion (10888 bp). The sequences of the internal oligos used for the PCR fusion were N1GR7 (5'-ATGTTGACACTTGAAGCCAC-3') found in intron 11 and GFP3' UTR (5'-TTCACCGTCATCACCGAAAC-3'). Transgenic animals were generated by injecting 40 ng/ $\mu$ l of the 11907 bp 5' *nca-1* PCR product with 40 ng/ $\mu$ l of the 10888 bp 3' *nca-1::GFP* fusion PCR product and 60 ng/ $\mu$ l of the coinjection marker *lin-15(+)* into TS384 *nca-2(gk5)III; nca-1(gk9)IV; lin-15(n765ts)X* hermaphrodites. The two halves of the *nca-1* construct overlap by 1.0 kb. The extrachromosomal arrays

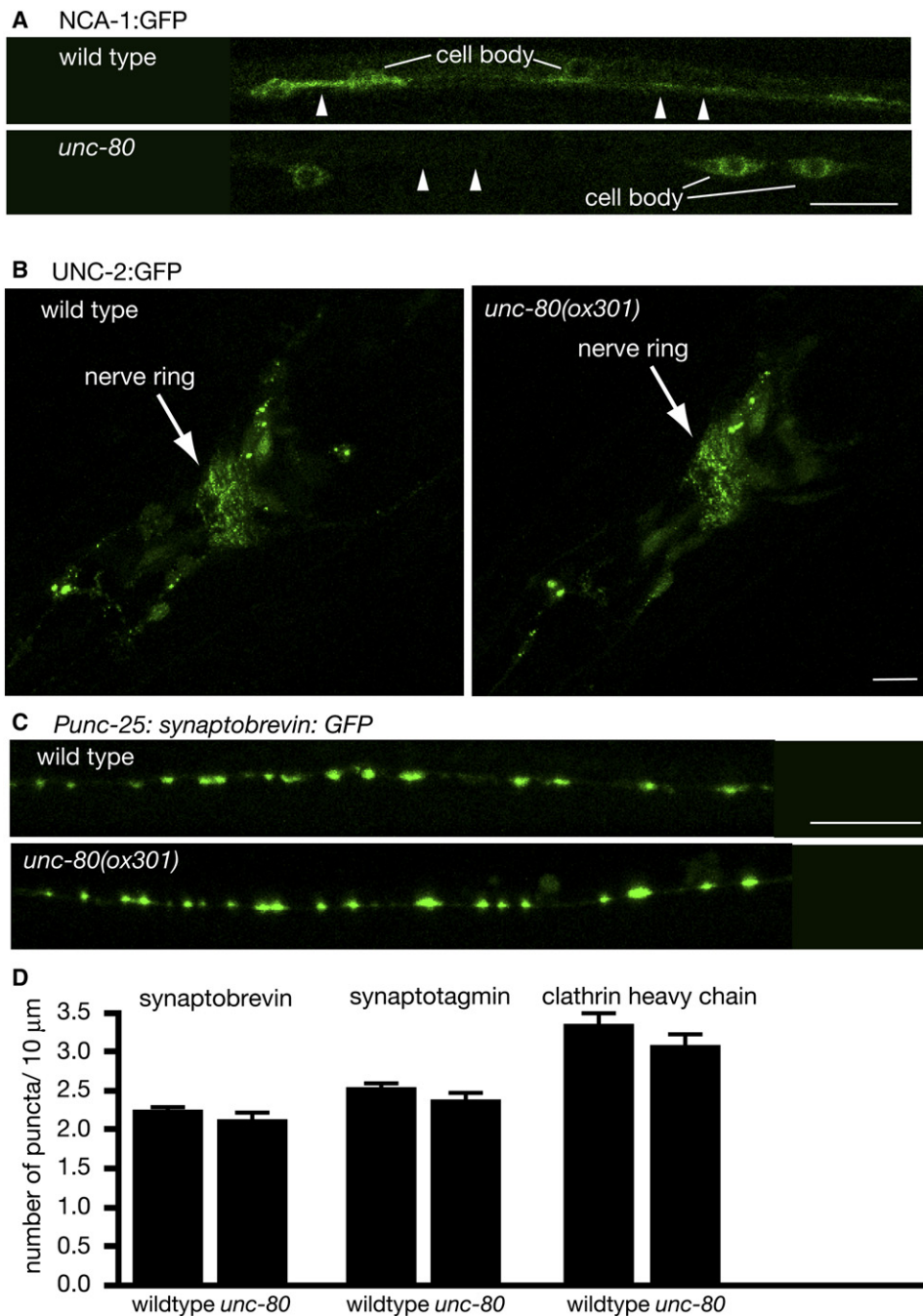


Figure S4. UNC-80 Is Required to Localize NCA-1 but Not Synaptic Proteins

(A) Ventral nerve cord of wild-type and *unc-80(ox301)* animals expressing NCA-1:GFP. Arrowheads point to the nerve cord, some cell bodies are indicated. Ventral cord is down.

(B) Head of wild-type and *unc-80(ox301)* animals expressing UNC-2:GFP. UNC-2:GFP is a rescuing construct and these genotypes are in an *unc-2(e55)* background to eliminate competition with the untagged protein. Axons in the nerve ring are marked by arrows. Right side of the nerve ring is shown.

(C) Example of localized GFP-tagged synaptobrevin (*Punc-25:GFP:synaptobrevin*) in the dorsal cord of wild-type and *unc-80(ox301)* animals, dorsal cord is facing up.

(D) Quantitative data of the dorsal cord, just posterior of the vulva, of wild-type and *unc-80(ox301)* animals expressing GFP-tagged synaptobrevin *Punc-25:GFP:synaptobrevin (nls52)*, *Punc-47:GFP-tagged synaptotagmin (oxIs224)*, and *Punc-47:GFP-tagged clathrin (oxIs174)* in GABA neurons. Dorsal cord of all scored animals is facing up. Number of puncta/10  $\mu\text{m}$  were scored. For synaptobrevin:GFP in wild-type: 2.2 puncta  $\pm$  0.7 SEM, in *unc-80(ox301)*: 2.0 puncta  $\pm$  0.1 SEM,  $p = 0.36$ , two-tailed, unpaired t test. GFP-tagged synaptotagmin in wild-type: 2.5 puncta  $\pm$  0.09 SEM, in *unc-80(ox301)*: 2.3 puncta  $\pm$  0.13 SEM,  $p = 0.28$ . GFP-tagged clathrin heavy chain in wild-type: 3.3 puncta  $\pm$  0.18 SEM, in *unc-80(ox301)*: 3.0  $\pm$  0.28 SEM,  $p = 0.39$ .

Scale bars represent 10  $\mu\text{m}$ .

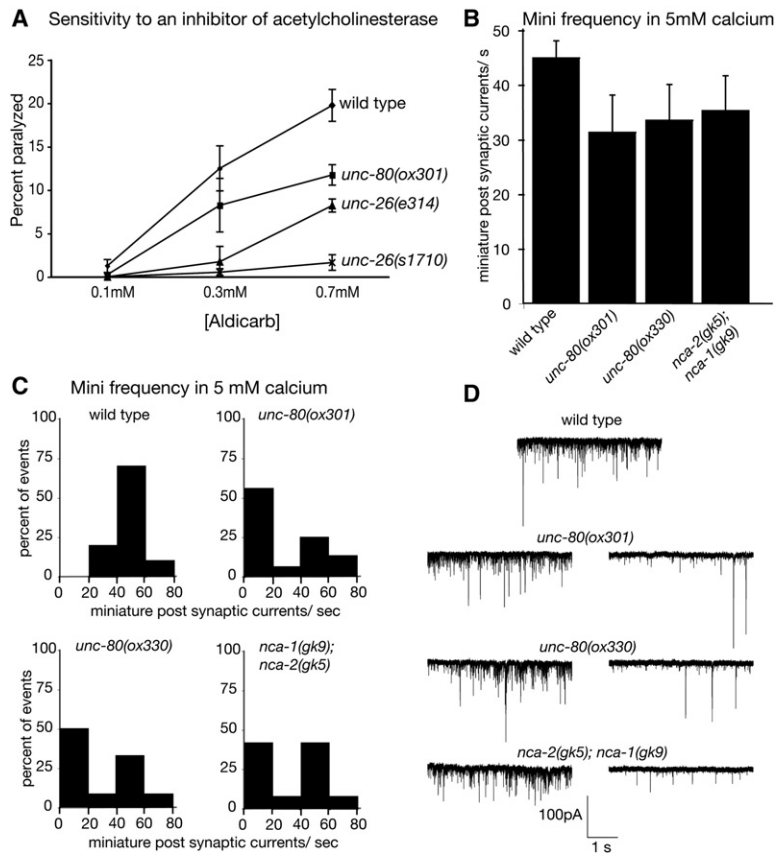


**Figure S5. Neurotransmission is Defective in the Absence of NCA Channel Function**

(A) Aldicarb assay for wild-type, *unc-80(ox301)*, *unc-26(e314)*, *unc-26(s1710)*. Aldicarb is an inhibitor of acetylcholine-esterase, which prevents degradation of acetylcholine in the synaptic cleft. Animals were exposed to differing concentrations of aldicarb for 6 hr before scoring. Animals were scored as paralyzed if their pharynx no longer pumped. Three assays were performed, each in triplicate, and scored blind.

(B) Frequency of minis in the presence of 5.0 mM external calcium from wild-type (44.9 ± 3.1 SEM, n = 10), *unc-80(ox301)* (31.3 ± 6.9 SEM, n = 16), *unc-80(ox330)* (33.5 ± 6.5 SEM, n = 12), *nca-2(gk5); nca-1(gk9)* (35.3 ± 6.4 SEM, n = 12). No significant difference between average mini frequencies was found in 5 mM external calcium when compared to the wild-type (*unc-80(ox301)*, p = 0.087, *unc-80(ox330)*, p = 0.346, and *nca-2(gk5); nca-1(gk9)*, p = 0.314).

(C) Frequency histograms plotted with a binning of 20 events/s showed a population exhibiting low mini frequency in *unc-80(ox301)*, *unc-80(ox330)*, and *nca-2(gk5); nca-1(gk9)*, but not in wild-type animals.

(D) Representative traces from wild-type, *unc-80(ox301)*, *unc-80(ox330)*, *nca-2(gk5); nca-1(gk9)* recorded in 5 mM calcium.

were integrated with  $\gamma$ -irradiation. The resulting strains were backcrossed six times to TS65 males and resulted in the generation of strain TS469.

#### ***Pnca-2::NCA-2::GFP Fusion***

The same strategy as for *nca-1* was used for *nca-2*. Again, a total of three PCR products were used. The first product (10769 bp) was generated with the sense primer N2GR1 (5'-TTATCCGGATTCC AGTTCGG-3'), approximately 3.4 kb upstream of the first exon (1a), and the antisense primer N2GR2 (5'-TCGTAAAGCCAATTCC ACG-3'), located in exon 6. The second product (8082 bp) was amplified with the sense primer N2GR3 (5'-TTTACGGGATCGATGGT ATC-3') and the antisense primer N2GR5 (5'-CTTTGGCCAA TCCCGGGATCATCACACAACGTCCACCAAG-3') that contained GFP sequence at its 5' end. The second product extended from the middle of exon 2 to the predicted stop codon. The third PCR product (1974 bp) amplified the GFP sequence from the plamid pPD95.75 with the sense primer N2GR6 (5'-CTTGGTGACG TTGTGTGATGATCCCGGGATTGGCCAAAG-3') that contained *nca-2* sequence at its 5' end and the primer GFP3'. Equimolar amounts of the 3' *nca-2* (second) and GFP (third) PCR products were then fused by PCR resulting in an in-frame carboxy-terminal translational fusion (9525 bp). The sequences of the internal oligos used for the PCR fusion were N2GR7 (5'-TTCGTATGCAATAATGGGTG-3') found in exon 4 and GFP3' UTR. The two injected halves of the *nca-2* construct overlap by 1.4 kb. Transgenic animals were isolated in the same manner as for *nca-1*, resulting in the generation of the *nca-2::GFP* strain TS465.

#### ***Punc-2::UNC-2::GFP Fusion***

The transgene used for rescuing *unc-2* was constructed by coinjecting three overlapping PCR fragments into *unc-2(e55)* animals. The PCR products included fragment 1 (12462 bp) generated with primer *unc2-37* (5'-TGGTTCGTTCTAACGTATCCG-3') and primer *unc2-38* (5'-GCTTCTGTGGCTTCGGCTTC-3'). Fragment 2 (10240 bp) was amplified with primers *unc2-43* (5'-TGAGTGGGGTTATCGGTAG-3') and *unc2-16* (5'-ACATTTTGACCCATGACTCC-3'). Fragment 3 (10098 bp) was a PCR fusion product generated with the procedure

previously described [S6] in which the gene for GFP was fused in-frame with *unc-2* preceding the predicted stop codon. The fusion was constructed by amplifying an 8189 bp with primers *unc2-15* (5'-GTTCTCCTGCTGAATGATAG-3') and *unc2-41*, which included GFP sequences at its 5' end (5'-CTTTGGCCAATCCCGGGATCAAC AATTGCCATCGAGGATCA-3'). GFP was amplified from the vector pPD95.75 (provided by A. Fire, Stanford University) with the primers *unc2-42* (5'-TGATCTCGATGGGCAATTGTTGATCCCGGGATTGCCAAAG-3') and GFP 3' (5'-ATCCGCTTACAGACAAGCTG-3'). Equimolar amounts of the *unc-2* and GFP products were then fused by PCR with the primers *unc2-44* (5'-CAATTTTGCAGAGGTACCGA-3') and GFPUTR (5'-TTCACCCGTCATCACCAGAAC-3'). Transgenic worms were generated by injecting *unc-2(e55) lin-15(n765ts)X* hermaphrodites with 30 ng/ $\mu$ l of each of the three PCR fragments and 50 ng/ $\mu$ l of pJM23 (*lin-15+*). The array in one of the established transgenic lines was integrated by  $\gamma$ -irradiation (*vals33*) and outcrossed six times with N2 males before crossing back into the *unc-2(e55)* mutant background, resulting in the strain TS337.

#### **Quantitative Fluorescence Microscopy**

Images were collected with a 63 $\times$  objective on a Zeiss Pascal Confocal microscope. Animals were immobilized with 2% phenoxypropanol. All images were taken with the same settings on the same day after the laser was allowed to stabilize for 30 min. Maximum intensity projections were analyzed with Image J software. For strains expressing synaptobrevin:GFP, synaptotagmin:GFP, and clathrin heavy chain:GFP, all images were taken at the same region of the dorsal cord with the animals turned with the dorsal nerve cord facing up. For *NCA-1::GFP* and *UNC-2::GFP* strains, images of the head were taken of animals lying on their left side with the right side facing up. Image series were taken from the center of the pharynx outwards through the entire right side of the nerve ring and the cuticle. Quantified images were of Z-series projections including all sections from the center of the pharynx through the nerve ring. The axons in the nerve ring were outlined for each animal and the average fluorescence value was calculated. The average fluorescence values

Table S1. Swimming Assay of Fainter Strains

	Number of Body Bends/s	Number of SEM	Number of Assays	p Value Compared to Mutant
Wild-type	2.06	0.07	5	
<i>unc-80(ox301)</i>	0.07	0.01	5	
<i>unc-80(ox330)</i>	0.14	0.02	5	
<i>unc-80(e1272)</i>	0.07	0.01	5	
<i>unc-80(ox301); oxEx1020<sup>a</sup></i> [ <i>unc-80 rescue</i> ]	1.32	0.05	5	<0.0001
<i>unc-80(ox301); oxEx1021<sup>a</sup></i> [ <i>unc-80 rescue</i> ]	1.53	0.02	5	<0.0001
<i>nca-2(gk5); nca-1(gk9)</i>	0.62	0.14	5	
<i>nca-2; nca-1;</i> <i>unc-80(e1272)</i>	0.16	0.06	5	0.17 (p value to <i>unc-80(e1272)</i> )
<i>nca-2; nca-1; vals46</i> [ <i>NCA-1::GFP</i> ]	1.74	0.2	5	0.0017
<i>nca-2; nca-1; vals41</i> [ <i>NCA-2::GFP</i> ]	1.42	0.04	5	0.0006

<sup>a</sup>*oxEx1020* and *oxEx1021* are independent extrachromosomal arrays isolated from coinjection of three overlapping PCR fragments amplified from genomic DNA.

were then averaged over six worms for both the control *vals46[NCA-1::GFP]* and experimental (*unc-80(ox301); vals46[NCA-1::GFP]*) strains. Similarly, the average fluorescence values were averaged over five worms for both the control *vals33[UNC-2::GFP]* and experimental (*unc-80(ox301); vals33[UNC-2::GFP]*) strains. Images shown in Figure 2 and Figure S4 are examples of images that were analyzed.

### Electrophysiology

Electrophysiological methods were adapted from previous studies [S8, S9]. Adult nematodes were glued (Histoacryl Bleue, B. Braun, Germany) along the dorsal side of the body to the surface of a plastic coverslip. A sharpened tungsten rod (A-M systems Inc, WA) was used to perform a lateral incision and to remove the viscera. The cuticle flap was glued back to expose the ventral medial body wall muscles and the preparation was treated by collagenase type IV (Sigma, MO) for 20 s at the concentration of 0.5 mg/mL.

Membrane currents were recorded in the whole-cell configuration of the patch clamp technique with an EPC-10 patch clamp amplifier (HEKA, Germany). Acquisition and command voltage were done with the HEKA Patchmaster software driving an LIH 1600 interface (HEKA, Germany). Data were analyzed and graphed with Mini Analysis (Synaptosoft, GA) and Microcal Origin software (Microcal Software Inc., MA). For all recordings, the membrane potential was maintained at a holding potential of  $-60$  mV. The resistance of recording pipettes was within 3–4.5 M $\Omega$ . Capacitance, resistance, and leak current were not compensated. All experiments were performed at room temperature.

The bath solution contained 150 mM NaCl, 5 mM KCl, 1 mM MgCl<sub>2</sub>, 10 mM glucose, 15 mM HEPES, and sucrose to 340 mOsm (pH 7.35). External CaCl<sub>2</sub> concentration was 0.5 or 5 mM, as indicated in each figure. For the low Ca<sup>2+</sup> solution, the concentration of MgCl<sub>2</sub> was increased to 4 mM as previously described [S10] in order to help stabilizing the membrane. The pipette solution contained 120 mM KCl, 20 mM KOH, 4 mM MgCl<sub>2</sub>, 5 mM N-tris [Hydroxymethyl] methyl-2-aminoethane-sulfonic acid, 0.25 mM CaCl<sub>2</sub>, 4 mM NaATP, 5 mM EGTA, and sucrose to 335 mOsm (pH 7.2).

### Electron Microscopy

Wild-type (N2), *unc-80(ox301)*, *nca-2(gk5); nca-1(gk9)*, *unc-26(s1710)*, *unc-26(s1710); unc-80(ox301)*, *nca-2(gk5); nca-1(gk9)* *unc-26(s1710)* adult nematodes were prepared in parallel for transmission electron microscopy similar to what was previously described [S11, S12]. In brief, 10 young adult hermaphrodites were placed onto a freeze chamber (100  $\mu$ m well of type A specimen carrier) containing space-filling bacteria, covered with a type B specimen carrier flat side down, and frozen instantaneously in the BAL-TEC HPM 010 (BAL-TEC, Liechtenstein). This step was repeated

for animals of all genotypes. Then, the frozen animals were fixed in Leica EM AFS system with 1% osmium tetroxide and 0.1% uranyl acetate in anhydrous acetone for 2 days at  $-90^{\circ}\text{C}$  and for 38.9 more hours with gradual temperature increases ( $6^{\circ}\text{C/hr}$  to  $-20^{\circ}\text{C}$  over 11.7 hr, constant temperature at  $-20^{\circ}\text{C}$  for 16 hr, and  $10^{\circ}\text{C/hr}$  to  $20^{\circ}\text{C}$  over 4 hr). The fixed animals were embedded in araldite resin following an infiltration series (30% araldite/acetone for 4 hr, 70% araldite/acetone for 5 hr, 90% araldite/acetone for overnight, and pure araldite for 8 hr). Mutant and control blocks were blinded. Ribbons of ultrathin (33 nm) serial sections were collected with ultracut 6. Images were obtained on a Hitachi H-7100 electron microscope with a Gatan digital camera. 250 ultrathin contiguous sections were cut, and the ventral nerve cord was reconstructed from two or more animals representing each genotype. Image analysis was performed with Image J software. The numbers of synaptic vesicles ( $\sim 30$  nm) in each synapse were counted, and their distance from presynaptic specialization and plasma membrane as well as the diameter of each was measured from cholinergic neurons VA and VB and the  $\gamma$ -aminobutyric (GABA) neuron VD. A synaptic profile was defined as the serial sections containing a dense projection.

### Supplemental References

- Davis, M.W., Hammarlund, M., Harrach, T., Hullett, P., Olsen, S., and Jorgensen, E.M. (2005). Rapid single nucleotide polymorphism mapping in *C. elegans*. BMC Genomics 6, 118.
- Kamath, R.S., Fraser, A.G., Dong, Y., Poulin, G., Durbin, R., Gotta, M., Kanapin, A., Le Bot, N., Moreno, S., Sohrmann, M., et al. (2003). Systematic functional analysis of the *Caenorhabditis elegans* genome using RNAi. Nature 421, 231–237.
- Nakai, K., and Horton, P. (1999). PSORT: a program for detecting sorting signals in proteins and predicting their subcellular localization. Trends Biochem. Sci. 24, 34–36.
- Letunic, I., Goodstadt, L., Dickens, N.J., Doerks, T., Schultz, J., Mott, R., Ciccarelli, F., Copley, R.R., Ponting, C.P., and Bork, P. (2002). Recent improvements to the SMART domain-based sequence annotation resource. Nucleic Acids Res. 30, 242–244.
- Schultz, J., Milpetz, F., Bork, P., and Ponting, C. (1998). SMART, a simple modular architecture research tool: identification of signaling domains. Proc. Natl. Acad. Sci. USA 95, 5857–5864.
- Hobert, O. (2002). PCR fusion-based approach to create reporter gene constructs for expression analysis in transgenic *C. elegans*. Biotechniques 32, 728–730.
- Clark, S.G., Lu, X., and Horvitz, H.R. (1994). The *Caenorhabditis elegans* locus *lin-15*, a negative regulator of a tyrosine kinase signaling pathway, encodes two different proteins. Genetics 137, 987–997.
- Richmond, J.E., and Jorgensen, E.M. (1999). One GABA and two acetylcholine receptors function at the *C. elegans* neuromuscular junction. Nat. Neurosci. 2, 791–797.
- Jospin, M., Jacquemond, V., Mariol, M.C., Segalat, L., and Allard, B. (2002). The L-type voltage-dependent Ca<sup>2+</sup> channel EGL-19 controls body wall muscle function in *Caenorhabditis elegans*. J. Cell Biol. 159, 337–348.
- S10. Lesa, G.M., Palfreyman, M., Hall, D.H., Clandinin, M.T., Rudolph, C., Jorgensen, E.M., and Schiavo, G. (2003). Long chain polyunsaturated fatty acids are required for efficient neurotransmission in *C. elegans*. J. Cell Sci. 116, 4965–4975.
- S11. Adler, C.E., Fetter, R.D., and Bargmann, C.I. (2006). UNC-6/Netrin induces neuronal asymmetry and defines the site of axon formation. Nat. Neurosci. 9, 511–518.
- S12. Rostaing, P., Weimer, R.M., Jorgensen, E.M., Triller, A., and Bessereau, J.L. (2004). Preservation of immunoreactivity and fine structure of adult *C. elegans* tissues using high-pressure freezing. J. Histochem. Cytochem. 52, 1–12.